ELSEVIER

Burns 31 (2005) 568–577

BURNS

www.elsevier.com/locate/burns

The relative thermal stability of tissue macromolecules and cellular structure in burn injury

F. Despa [a], D.P. Orgill [b], J. Neuwalder [b], R.C. Lee [a,*]

[a] *Department of Surgery, MC6035, The University of Chicago, Chicago, IL 60637, USA*
[b] *Department of Surgery, Brigham and Woman's Hospital, Harvard Medical School, Boston, MA 02115, USA*

Abstract

When tissue is subjected to higher than physiological temperatures, protein and cell organelle structures can be altered resulting in cell death and subsequent tissue necrosis. A burn injury can be stratified into three main zones, coagulation, stasis and edema, which correlate with the extent of heat exposure and thermal properties of the tissue. While there has been considerable effort to characterize the time–temperature dependence of the injury, relatively little attention has been paid to the other important variable, the thermal susceptibility of the tissue. In the present study, we employ a standard physical chemistry approach to predict the level of denaturation at supraphysiological temperatures of 12 vital proteins as well as RNA, DNA and cell membrane components. Melting temperatures and unfolding enthalpies of the cellular components are used as input experimental parameters. This approach allows us to establish a relation between the level of denaturation of critical cellular components and clinical manifestations of the burn through the characteristic zones of the injury. Specifically, we evaluate the degree of molecular alteration for characteristic temperature profiles at two different depths (Mid-Dermis and Dermis-Fat interface) of 80 °C; 20 s contact burn. The results of this investigation suggest that the thermal alteration of the plasma membrane is likely the most significant cause of the tissue necrosis. The lipid bilayer and membrane-bound ATPases show a high probability of thermal damage (almost 100% for the former and 85% for the latter) for short heat exposure times. These results suggest that strategies to minimize the damage in a burn injury might focus on the stabilization of the cellular membrane and membrane-bound ATPases. Further work will be required to validate these predictions in an in vivo model.

Keywords: Burn; Molecular stability; Protein denaturation; Membrane poration; Model

1. Introduction

Thermal injury can be better understood by examining the behavior of cellular components at supraphysiological temperatures. Which proteins and organelles are most vulnerable to heat injury and which play critical roles in cell viability? Biomolecules optimally perform their function when they are in specific three-dimensional conformations. High temperatures cause alteration in conformations often leading to irreversible processes (denaturation), which affect cell viability and trigger cell death. Because the functional structure of each protein and organelle is unique, so is its vulnerability to denaturation at high temperatures.

Thermal denaturation of proteins and disruption of organelles involve intramolecular restructuring and intermolecular reorganization. The kinetics of these processes depend on the strength of the chemical bonds, density, solvent and interactions with adjacent molecules such as molecular chaperones. Despite the fact that the kinetics of thermal damage for each biomolecular structure depend on multiple factors in the chemical environment, experimental observation of burn injury suggests that the burn injury process can be described by a unique exponential equation [1–7]. Almost five decades ago Moritz and Henriques determined the energetics of a burn injury by quantifying the time–temperature relationship for scald burning of forearm skin [2]. Injury was defined by observing skin blistering in contact with hot water. Blistering occurred after only 5 s for water at 60 °C, whereas water at 43 °C took 6 h to form a blister. Their experimental data display an Arrhenius-type of

* Corresponding author.
E-mail address: r-lee@uchicago.edu (R.C. Lee).

0305-4179/$30.00
doi:10.1016/j.burns.2005.01.015

behavior, which is usually observed in thermally activated chemical reactions.

What is the solution to this apparent dilemma? Possibilities include statistical arguments such as the "central limit theorem", which states that a process that depends on an infinite number of subordinate different processes behaves like a single Arrhenius process. Thus, burn injury necrosis could involve a vast number of molecular injuries. Another hypothesis is that lethal burn injury is dominated by only a few molecular processes. The latter could be valid if those processes are critical to cell survival, e.g., denaturation of critical cellular structure or protein. If this hypothesis is correct, development of therapeutics that effectively intervene in the injury process and limit burn injury could be useful for burn treatment.

To address the validity of the critical process hypothesis, it is necessary to establish a correspondence between the extent of molecular changes in tissues and tissue manifestations following heat exposure. Because of the lack of observation of protein dynamics in cells, we must rely on calorimetric measurements of protein denaturation in solution to infer the behavior of the cellular components at supraphysiological temperatures. The typical approach for modeling intracellular kinetics is to correct the chemical kinetic rates measured in dilute solution for various effects such as molecular crowding and heating rate. Although the results can be suggestive, such an approach provides only a crude approximation to the complex burn injury. Potentially important interaction biomolecules such as molecular chaperones, immune components and cytokines, which may add stability in response to thermal injury, were disregarded. Under such circumstances, the purpose of this research is to identify a few candidate proteins and cellular structures that could be the most critical determinators of tissue survival in burn trauma.

2. Methods

2.1. Bio-heat transfer rate

A typical burn is divided in to zones of injury reflecting the fact that the temperature profile is non-uniform in the tissue. The bio-heat transfer equation [8], which accurately predicts the spatial dependence of the temperature history, states that the rate of temperature change in a small volume of tissue is equal to the sum of the heat transfer from the surrounding tissues (conduction) and the heat transfer from blood perfusing the block (see Fig. 1). Usually, a term due to metabolic heat generated by the cells is included in the model. However, such a contribution is negligible for thermal injuries that occur over a short period of time. The mathematical formulation of the bio-heat transfer model reads

$$\rho c \frac{\partial T}{\partial t} = \nabla k \nabla T + \omega_b \rho_b c_b (T - T_b) \quad (1)$$

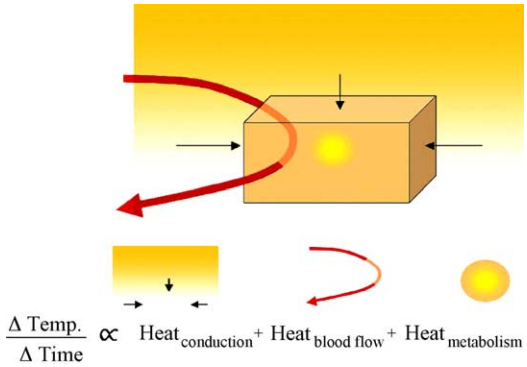

Fig. 1. Bio-heat transfer equation defines the rate of temperature change in a small volume of tissue.

ρ, c and k denote density, heat capacity and conductivity of tissue, 'b' is an index for physical properties of blood and ω_b is the normalized blood perfusion of tissue. Experimental observation of blood perfusion has shown that heat transfer occurs primarily at the arteriole level and not at the capillary. This may explain why there can often be sparing of thermal injury around some small blood vessels [9].

Solutions of Eq. (1) describe the temperature distribution in tissues. Based on these temperature profiles and knowing the temperature dependence of the equilibrium constant (K) of the folding/unfolding process for each cellular component, we can model the heat damage accumulation at the molecular level, e.g., we can quantify explicitly the level of denaturation of various cellular components at different depths in the tissue. The theoretical basis of this approach is the focus of the following section.

2.2. Energetics of molecular denaturation

At body temperature, proteins are in native conformations that allow them to perform their designated functions. At supraphysiological temperatures, proteins are driven towards unfolded conformations (Fig. 2). In unfolded conformations, many proteins tend to form stable insoluble aggregates. Aggregation is a major source of irreversibility of protein unfolding when the temperature returns to normal. A common example is seen when cooking an egg. When the temperature of the egg white reaches approximately 60 °C the translucent viscous solution turns irreversibly to a solid white gel.

Protein unfolding occurs even at body temperature. Typically, cells have a certain capacity to endure or repair this damage [10]. A basic model for describing structural changes of proteins between various conformations requires an explicit formulation of the driving thermodynamic forces involved in the process [11–14]. It has been shown [15,16] that the ability of a molecule to accomplish a particular chemical process is reflected by the change of its free energy. The thermodynamic state of a molecule depends on all internal and external forces acting on it and temperature. As

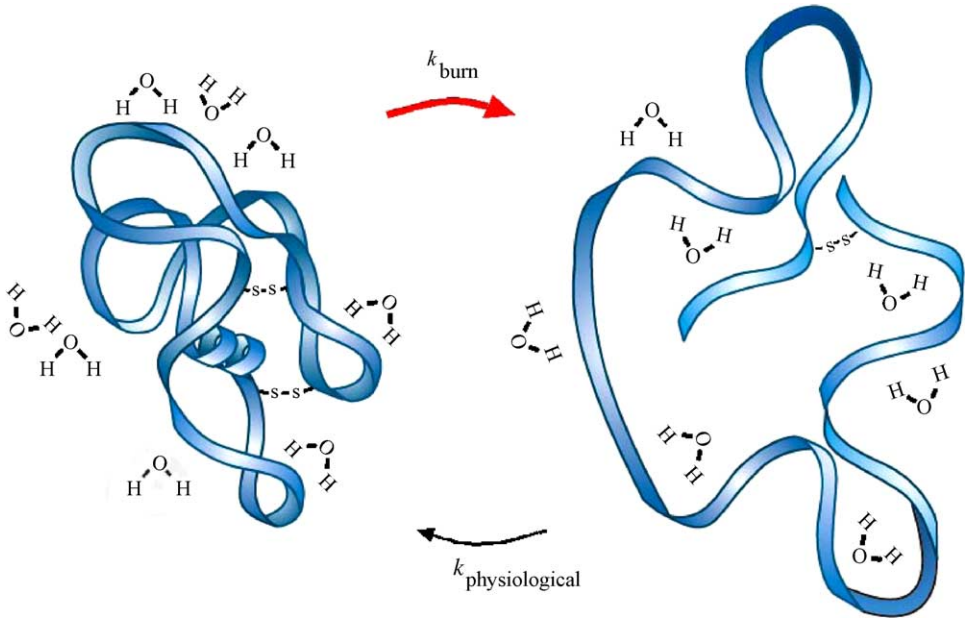

Fig. 2. Proteins unfold in response to heating; in many cases this process is irreversible.

temperature increases, the protein loses the ability to maintain its native conformation (N) and starts the transition towards the unfolded state (U). When the temperature rises above the "melting temperature" (T_m), the protein achieves enough energy to unfold and refold (N ↔ U) at equal rates. It can be shown that the functional relation between unfolding (k_u) and refolding (k_f) rates at any temperature depends on T_m as

$$K \equiv \frac{k_u}{k_f} = \exp\left(-\frac{\Delta H}{RT}\left(1 - \frac{T}{T_m}\right)\right), \quad (2)$$

where ΔH represents the enthalpy change between the unfolded and native states, and $R \cong 8.315\ \mathrm{J\ K^{-1}\ mol^{-1}}$ is the molar gas constant. The fraction of unfolded molecules f_d at each temperature T of the temperature profile $T(t)$ is given by

$$f_d = \frac{K(T)}{1 + K(T)}. \quad (3)$$

In situ thermal protein unfolding is approximately an irreversible process [17]. Under conditions in which cells are thermally damaged, cellular components in final denatured states (D) are unable to "return" to N or U

$$N \leftrightarrow U \rightarrow D.$$

The U → D conversion is described by a kinetic rate k_d in the general Lumry-Eyring model [18]. The two limiting cases of the general model depend upon whether the unfolded protein refolds N ↔ U or undergoes the irreversible alteration U → D. If the irreversible alteration is faster than refolding, then the rate of overall denaturation (and, therefore, the calculated rates k_u and k_f) becomes independent of the rate of the irreversible step. Thus, $f_d(t)$ is a direct measure of the extent of denaturation of a specific cellular component, which can be monitored in time given ΔH, T_m and the time course of the temperature $T(t)$.

Many of the values of the thermodynamic parameters T_m and $\Delta H(T)$ of the folding/unfolding processes can be found in the differential scanning calorimetry literature (DSC) [19]. DSC measurements of proteins are performed usually at low concentrations to avoid aggregation during unfolding. However, in the cytoplasm of cells, a large number of soluble and insoluble macromolecules coexist at different concentrations, sometimes at very high concentrations depending on physiological and environmental conditions. The concentration of macromolecules in cytoplasm varies in the range of 80–200 mg/ml [20]. The work required for a protein to unfold in such a crowded solution is much greater than required for unfolding in a dilute solution. This difference is due to volume exclusion [21] which can lower the equilibrium constant K (see Eq. (2)) of the protein folding/unfolding process by up to one order of magnitude. Crowding affects the value of the melting temperature of the protein [22,23]. For example, the melting temperature of *actin* increases by approximately 5 °C in the presence of 100 mg/ml PEG-6000, a non-ionic surfactant [24]. Volume exclusion also occurs due to confining proteins in small compartments. Experiments have shown that proteins encapsulated in small pores in hydrated silica glasses have an enhanced stability when heated [25]. Minton derived a correction for the melting temperature of the protein in solution to account for volume exclusion effects [22], $\Delta T_m \cong 2.303 \frac{R}{\Delta H_m} \Delta \log K$. This equation states that any isothermal variation of the equilibrium reaction constant K changes the temperature at which half of the proteins are denaturated. Here, ΔH_m is the enthalpy of unfolding at the melting temperature T_m as determined under the usual conditions of DSC experiments [22]. Therefore, we include in the present computation corrections to the DSC data to account for the crowding effect in cells. We will consider a

Table 1
Thermodynamic parameters T_m and ΔH_m and corresponding references for each molecule investigated in the present work

	ΔH_m (kJ)	T_m (°C)	Reference	T_m^* (°C)
Lipid bilayer	290	41.6	27	45.6
Spectrin	197.19	66	29	72.8
NKP	490	54.5	30	57
PMCP	224	47.4	31	52.8
SRCP	411	60	32	63.1
DNA	314	55.5	33	59.5
RNA	326	58.4	34	62.3
Histone	259.83	47.2	35	51.8
Cytochrome *c*	338.9	60	36	63.8
ATP synthesis *e*	539.74	57.5	37	59.8
F actin	782.41	67	38	68.7
Myosin	355.64	53.7	39	57.2
Tubulin	627.6	55.8	40	57.8
ApoCaM	332	60	41	63.9
Collagen	289	58	43	62.4

In the last column, T_m^* values represent estimations for the melting temperatures corrected for crowding effects in the cell (see the text).

correction ΔT_m corresponding to an average cosolute concentration of about 140 mg/ml ($\Delta \log K \cong 0.75$) [22].

Another important factor is that the heating rate in the DSC measurements affects protein dynamics. Both T_m and ΔH_m depend on the heating rate. For example, collagen unfolds at 58 °C when the temperature is increased at 1 °C/min and at 60 °C degrees when the temperature increase is 2 °C/min [26]. Generally, the relationship between scanning rate and the temperature of the endotherm maximum is logarithmic [26]. Most of the results in DCS measurements were obtained at a heating rate of 1.5 °C/min. The heating rate in a real burn injury can be much higher and, consequently, the present description might be distorted. However, because tissues have an important thermal inertia, which slows heat transfer, we can assume that the processes at the molecular level occur on a time scale for which the present thermodynamic approach is still valid.

2.3. Computer simulations

We performed an exhaustive search of the calorimetric database and selected melting temperatures and unfolding enthalpies for 12 vital proteins as well as RNA, DNA and cell membrane components. We have systematically chosen reported data at the pH as close as possible to the physiological value, i.e. pH ≅ 7. The buffer conditions are specified in the literature references. In Table 1, we

Table 2
Expected percent denaturation f_d (%) for selected proteins and membrane structure after exposure for 20 s to various temperatures between 40 and 66 °C

Molecule	Temperature (°C)													
	40	42	44	46	48	50	52	54	56	58	60	62	64	66
lipid bilayer		0.02	2	74	100									
spectrin													0.02	2
NKP								0.01	4	95	100			
PMCP						1.3	23	87.4	100					
SRCP												7	88	100
DNA										5	72	100		
RNA											1	35	96	
histone						3	59	98	100					
cytochrome c												3	59	89
ATP synthesis e										1	62	100		
F actin														
myosin									6	86	100			
tubulin									1	69	100			
apoCam												3	55	92
collagen											2	33	93	100

display the values of thermodynamic parameters T_m and ΔH_m along with the corresponding references for each molecule. Also, we include in Table 1 expected values of T_m^* for the melting temperatures of proteins in situ, which are DSC melting temperatures corrected for the crowding effect $T_m^* = T_m + \Delta T_m$, as described above.

Numerical simulation of protein thermodynamics and corresponding graphics were performed with Mathematica 4 (Wolfram Resesarch, Champaign, IL). The characteristic diagrams of protein denaturation over the temperature range relevant for burn injuries (see Tables 2–4) are discussed below.

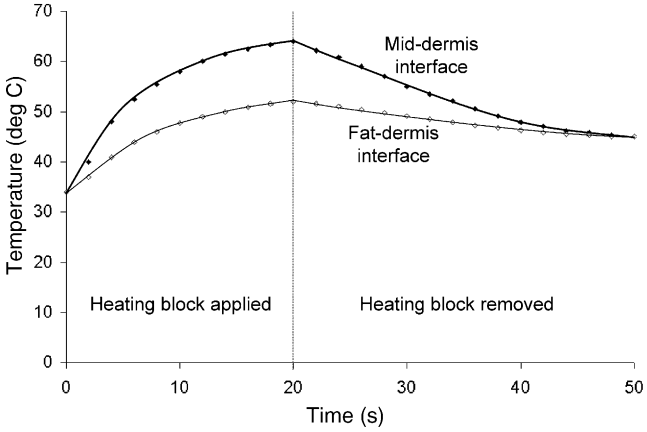

Fig. 3. Temperature profiles at Mid-Dermis and Dermis-Fat interface for a 20-s contact burn (reproduced from Ref. [8]).

3. Results

Using the present approach, we computed the percent denaturation (f_d) for the selected cellular components after being subjected to various 20 s imposed temperatures ranging between 40 and 64 °C (see Table 2). In general, temperatures below 44 °C are well tolerated by all the cellular components except the lipid bilayer. The lipid bilayer achieves a 2% denaturation for a temperature increase of only 2 °C, from 42 to 44 °C. An increase of the temperature to 45 °C leads to a rapid denaturation of this membrane component.

Next, we characterized the behavior of selected cellular components for the specific conditions of 80 °C; 20 s contact burn (see Ref. [8] for experimental details). We estimated the time–temperature relationship of the overall denaturation f_d (see Eq. (3)) for each cellular component at the Mid-Dermis (Table 3) and Fat-Dermis (Table 4) interfaces (see Fig. 3). We proceed from the plasma membrane through the cytoplasm to the nucleus so that the level of denaturation of many diverse proteins produced by elevated temperatures can be clearly shown.

Table 3
Expected percent denaturation f_d (%) vs. time for various cellular components corresponding to Mid-Dermis temperature profile (see, Fig. 3)

Molecule	time (s)																	
	3	4	5	6	7	8	9	10	11	12	13	14	15	16	17	18	19	20
lipid bilayer	0.3	98	100															
spectrin																		
NKP						1	35	95	100									
PMCP				13	74	97	100											
SRCP												1	5	10	25	41	65	86
DNA							1	11	43	78	93	100						
RNA										2	6	17	36	58	75	86	92	95
histone			4	16	94	100												
cytochrome c													3	8	15	21	40	54
ATP synthesis e								1	17	74	96	100						
F actin																		
myosin						6	55	94	100									
tubulin							11	92	100									
apoCam													3	7	14	24	37	50
collagen										2	7	18	34	53	69	81	88	92

Table 4
Expected percent denaturation f_d (%) vs. time for various cellular components corresponding to the temperature profile at the Fat-Dermis interface (see, Fig. 3)

Molecule	Time (s)																	
	3	4	5	6	7	8	9	10	11	12	13	14	15	16	17	18	19	20
lipid bilayer				2	23	79	97	100										
spectrin																		
NKP																		
PMCP												2	3	5	8	13	18	25
SRCP																		
DNA																		
RNA																		
histone											2	4	9	16	26	38	50	61
cytochrome c																		
ATP synthesis e																		
F actin																		
myosin																		
tubulin																		
apoCam																		
collagen																		

3.1. Plasma membrane

The plasma membrane defines the boundaries of the cell and is in immediate contact with the environment. Therefore, it can be expected a priori that any alteration of the plasma membrane has important consequences on cellular activity.

3.2. The lipid bilayer

Three major types of amphipathic molecules constitute the plasma membrane: phospholipids, cholesterol and glycolipids. These form bilayers with the hydrophobic tails sandwiched between the hydrophilic head groups and present self-assembling and self-sealing properties. Calorimetric measurements of the characteristic temperature T_m at which the gel and liquid crystalline phases of a lipid bilayer are equi-probable ($f_d = 50\%$) yielded a value just above the physiological temperature, $T_m = 41.6\ ^\circ C$. Although the natural confinement of the lipid bilayer by other membrane constituents may enhance T_m by a couple of degrees, the present approach predicts relatively significant denaturation of this system to occur between 42 and 45 °C. Thus, the lipid bilayer achieves a 2% denaturation for a temperature increase of only 2 °C, from 42 to 44 °C. Further increase of the temperature to 45 °C leads rapidly to 50% denaturation of this membrane component. These predictions correlate well with the experimental observations of cell membrane permeability changes [27]. Accordingly, calcein leakage increases rapidly over 45 °C [27] and hyperthermia-induced blebbing correlates with cell death at 45.5 °C [28]. In the context of the present results, the lipid bilayer seems to represent the critical target for the cell killing.

Fig. 4 illustrates the lipid bilayer's rapid denaturation for a specific temperature history which reaches values above 45 °C. Here, f_d is displayed against time for the temperature profile at Mid-Dermis in 80 °C; 20 s contact burn. The lipid bilayer appears to reach complete denaturation ($f_d = 100\%$) in the first 5 s of the injury process at 1.04 mm depth into skin and in 10 s at 2.50 mm (see Tables 3 and 4). These results suggest that plasma membrane integrity is easily compromised when cells are subjected to supraphysiological temperatures [27].

3.3. Membrane proteins

In human red blood cells three types of proteins (spectrin, glycophorin and band III) account for more than 60% (by weight) of the total membrane protein. Spectrin is the major compound of the membrane protein mass (30%) [29]. In Table 2, we present the estimated level of unfolding at high temperatures of *spectrin*. Relative to other biomolecules, spectrin is thermally stable, as less than 3% unfolds at 66 °C.

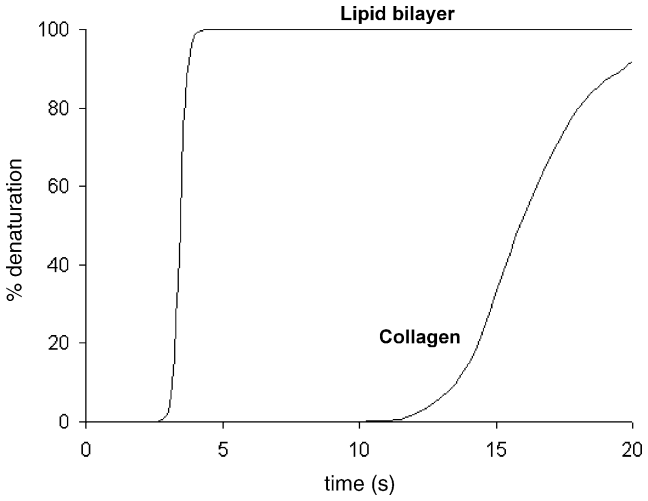

Fig. 4. The evolution in time of the fraction of denaturated lipid bilayer f_d at Mid-Dermis corresponding to the temperature profile in Fig. 3. The same for collagen molecules.

We also estimated the denaturation level of two membrane-bound ATPases: Na^+/K^+ pump and Ca^{2+} pump. The Na^+/K^+ pump (NKP) maintains the electrostatic potential across the plasma membrane. Its thermal denaturation thermogram displays the unfolding of three cooperative domains with midpoint transition temperatures $T_{m1} = 47.6\ ^\circ C$, $T_{m2} = 54.5\ ^\circ C$ and $T_{m3} = 58.5\ ^\circ C$ [30]. Apparently, thermal unfolding of the first domain has no effect on ATP activity [30]. The second temperature domain is most likely associated with a significant perturbation of the ATP activity at high temperatures. We computed the denaturation levels of the NKP at high temperatures by using $T_{m2} = 54.5\ ^\circ C$ as the experimental characteristic transition temperature. The results are displayed in Tables 2–4. Ca^{2+} *pump* transports Ca^{2+} outward to extracellular medium and sarcoplasmic reticulum (SR). Plasma membrane Ca^{2+} pump (PMCP) is very susceptible to heat and characterized by a low experimental transition temperature ($T_m = 47.4\ ^\circ C$) [31]. Elevated temperatures may lead to the formation of intramembraneous protein aggregates associated with irreversible functional alterations. By looking in Table 2, we can see that the fractions of denaturation f_d of these membrane-bound proteins achieve significant values (around 50%) just above physiological temperature ($\approx 50\ ^\circ C$). This observation suggests a correlation between the above effects and hyperthermic killing. It is interesting to note that the sarcoplasmic reticulum Ca^{2+} pump (SRCP) is more thermally stable than PMCP. This can be inferred by looking at the experimental parameter T_m ($\approx 13\ ^\circ C$ higher for SRCP) [32]. SRCP is the only major protein in the *SR* and accounts for about 90% of SR protein.

3.4. Nuclear proteins

Prevention of gene transcription or translation will lead to cell death. Data is available for thermal stability of certain DNA segments. In Tables 2–4, we present predicted values for the thermal alteration of the duplex sequences dGCATAATACGT/d of DNA [33] and ACCUUUGC of RNA [34]. Although DNA and RNA are generally assumed to maintain their structural stability at elevated temperatures, our prediction is that small portions of these biomolecules can easily be altered by heat. For example, the above sequence of DNA, which is the largest analyzed experimentally [33], shows a 50% probability of unfolding at a temperature about 59 °C.

We also predict values for thermal denaturation of histone [35], one of the most numerous chromosomal proteins (6.0×10^7 of each type per cell). Histone plays an important role in reactions that involve the genome. Apparently, the thermal stability of this protein is significantly lower than those of DNA and RNA (e.g., denaturation at Mid-Dermis is complete in the first 9 s of a 80 °C; 20 s contact burn).

3.5. Mitochondrial proteins

Mitochondria occupy a substantial fraction of the cytoplasm of virtually all eukaryotic cells. They carry out most cellular oxidation and produce the bulk of the cell's ATP. Energy is harnessed by an electron-transport chain embedded in the mitochondrial inner membrane, which creates a transmembrane electrochemical proton gradient by pumping protons out of the matrix. Tables 2–4 present general predictions for thermal denaturation of two main proteins involved in this process: *cytochrome c* [36], which plays the therminal role in the respiratory chain and ATP synthetase [37] which makes ATP in the matrix. Apparently, these proteins are characterized by a higher thermal stability than others we have discussed above, e.g., they remain intact below 60 °C.

3.6. Cytoskeletal proteins

Properties of shape, internal organization and movement depend on complex networks of protein filaments in the cytoplasm that form the cell's cytoskeleton. The two most important structural elements within a cell are actin filaments (microfilaments) and microtubules. We investigated the thermal denaturation of the components of microfilaments (F actin [38] and myosin [39]) and tubulins [40], which constitute microtubules.

Actin, which significantly populates the native state even for a third-degree burn (almost 40%), displays considerable thermal stablility. In comparison, the much lower stability of *myosin* is striking; *myosin* appears very susceptible to heat (the probability to unfold is almost unity at $T = 60\ ^\circ C$).

The movement of actin and myosin in muscle cells is regulated by a *calmodulin*-Ca^{2+} switch. Tables 2–4 also present predictions for the denaturation level of calmodulin (apoform) at elevated temperatures. Calmodulin is fairly stable at elevated temperatures, and its stability can be further increased by the presence of Ca^{2+} (holoform) [41].

3.7. Collagen

The collagens are a family of fibrous proteins that form the extracellular matrix. They are the most abundant in mammals, constituting 25% of their total protein. The central feature of all collagen molecules is a stiff, triple-stranded helical structure. Apparently, the helical structure of the collagen molecule is not stable at the physiological temperature [42]. However, it has been suggested that the thermal instability of collagen is essential for fibrillogenesis. Fiber formation yields stabilization of collagen helices and prevents further unfolding; collagens undergo folding/unfolding processes as needed, giving fibers strength and elasticity. At high temperatures, the triple helical structure of collagen becomes more and more altered and rapidly becomes extinct over $T_m \cong 58\ ^\circ C$ [43]. Tables 2–4 display relevant information about the thermal stability of collagens. In Fig. 4 compares the dynamics of denaturation of collagen molecules at Mid-Dermis with that corresponding to the lipid bilayer.

4. Discussion

The present approach uses calorimetric data to predict the expected level of protein denaturation at temperatures shown to produce thermal injuries. Generally, as discussed above, calorimetric measurements depend on the heating rate. Most of the calorimetric data are recorded at a heating rate of 90 °C/h, which is considered slow enough to allow the structural equilibrium. Nevertheless, thermodynamic characterization of a protein in vitro only approximates the denaturation that would take place within a cell. Although buffer conditions can be prepared for a wide range of pHs, including the physiological pH, they can not substitute the cell environment [44]. As seen in Table 1, crowding effects can substantially increase the thermal stability of the cellular components.

In this context, it is interesting to compare the time–temperature dependence of a second-degree burn with the time–temperature plot for 50% denaturation of the lipid bilayer (see Fig. 5). It is not surprising that the curves are very different as they reflect the time required to observe very different responses. Although in a second-degree burn, an immediate change in transport properties is observed within microseconds, microvascular and immunological responses may take hours to manifest. Besides, the reference temperature in Moritz and Henriques [2] experiments is measured at the surface of the skin (at the level of stratum corneum), which is different from the temperature inside the tissue (as described by the bio-heat transfer Eq. (1)). The actual temperature affecting the viability of cell below the stratum corneum is lower. Therefore, Moritz and Henriques [2] data are shifted up on the temperature scale, which makes difficult a comparison with the time–temperature dependence of 50% denaturation of the lipid bilayer.

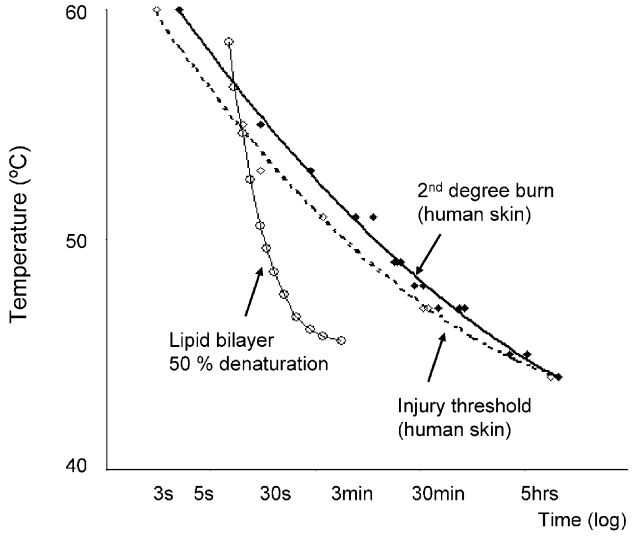

Fig. 5. Time vs. temperature relationship of 50% denaturation for lipid bilayer compared to the time–temperature data for a second-degree burn (data reproduced from Moritz and Henriques [2]). Moritz and Henriques used $\frac{d\Omega}{dt} = A \exp\left(-\frac{E}{RT(t)}\right)$ to describe the tissue destruction (Ω) in time (t). Viable cells suffer irreversible transformation passing over a denaturation energy barrier $E = 627\ kJ\ mol^{-1}$ (A is a scaling factor, $A = 3.0 \times 10^{98}\ s^{-1}$). Lipid bilayer data were obtained from Eq. (3) for a step-rise temperature in time of the form $T = 37\ ^\circ C + \Delta T(1 - e^{t/0.5})$, with ΔT between 8.6 and 21.6 °C. We imposed that 50% denaturation of the lipid bilayer to be reached at $T = 45.6\ ^\circ C$ on a time scale of minutes, as described by Borrelli et al. [28].

The present study shows that the proportion of unfolded protein increases dramatically at supraphysiological temperatures. At temperatures above 60 °C most tissue proteins are denatured with probabilities approaching unity. F actin seems to be a very stable protein at elevated temperatures with a probability of unfolding above the temperature range we considered in the present study. In addition to actin, cells of high thermal stability contain heat-shock proteins (Hsps), which are assumed to act as molecular chaperones to assist in refolding denatured proteins. Hsp25 and Hsp27 have a midpoint transition temperature of $T_m = 69.9\ ^\circ C$ [45], higher than that corresponding to F actin, for example. We can predict that Hsps can exist in functional form of 80% even above 75 °C. However, results of this study suggest that above 45 °C the cell membrane breakdown is so extensive that it is improbable that Hsps occur in high enough concentration to be an effective protector against cell disruption.

Our calculations find the lipid bilayer and membrane-bound ATPases to be the proteins most predisposed to thermal denaturation. Thus far, the present study suggests that the thermal alteration of the plasma membrane is likely to be the most significant cause of the tissue necrosis. This hypothesis correlates with the observation that edema is considered to be the first evidence of thermal injury in tissue. This edema is likely due to early disturbances in the cell membrane or cell membrane ion pumps (NKP). In many cases it appears that these cells can recover from this injury,

i.e., most first-degree burns heal. Temperatures above the first-degree burn threshold lead to irreversible damage to the cell membrane or other macromolecules and yield a critical injury.

Finally, the present approach suggests the need for further exploration of possible molecular mechanisms relating minor T_m changes to major connective tissue pathology caused by such changes. For instance, our mathematical simulations show that an increase in T_m by 1 °C changes the rate of protein unfolding significantly. Understanding the regulation of these processes may lead to clinical strategies for limiting the devastating development of the injury after the thermal insult of the tissue stopped.

Acknowledgements

The research presented here has been partly supported by the National Institutes of Health, grants R01 GM61101 (RCL) and R01 GM64757 (RCL), and The Electric Power Research Institute (RCL).

References

[1] Lepock JR. Cellular effects of hyperthermia: relevance to the minimum dose for thermal damage. Int J Hyperthermia 2003;19:252–66.
[2] Moritz AR, Henriques FC. Studies of thermal injury. Am J Pathol 1947;23:695–720.
[3] Diller KR. Analysis of skin burns, in heat transfer in medicine and biology: analyses and applications, vol. 2. NY: Plenum, 1985. p. 85–134.
[4] Diller KR. Modeling of bio-heat transfer process at high and low temperatures. Adv Heat Transfer 1992;22:157–357.
[5] Diller KR, Pearce JA. Issues in modeling thermal alterations in tissues. Ann N Y Acad Sci 1999;888:153–63.
[6] Lee RC, Astumian RD. The physico-chemical basis for thermal and non-thermal burn injury. Burns 1996;22:509–19.
[7] Lee RC, Zhang D, Hannig J. Biophysical injury mechanisms in electrical shock trauma. Annu Rev Biomed Eng 2000;2:477–509.
[8] Orgill DP, Solari MG, Barlow MS, O'Connor NE. A finite-element model predicts thermal damage in cutaneous contact burns. J Burn Care Rehabil 1998;19:203–9.
[9] Valvano JW, Diller KR, Pearce JA. Bio-heat transfer: in crc handbook of heat transfer. Frank Kreith; 2000. p. 4114–87.
[10] Johnson HA, Pavalec M. Thermal noise in cells: a cause of spontaneous loss of cell junction. Am J Pathol 1972;69:119–30.
[11] Despa F, Berry RS. Inter-basin dynamics on multidimensional potential surfaces. I. Escape rates on complex basin surfaces. J Chem Phys 2001;115:8274–9278.
[12] Despa F, Berry RS. Inter-basin dynamics on multidimensional potential surfaces, kinetic traps. Eur Phys JD 2003;24:203–6.
[13] Despa F, Fernàndez A, Berry RS, Levy Y, Jortner J. Inter-basin motion approach to dynamics of conformationally constrained peptides. J Chem Phys 2003;118:5673–82.
[14] Despa F, Berry RS. Relaxation dynamics in the presence of unequally spaced attractors along the reaction coordinate. Eur Phys JD 2001;16:55–8.
[15] Hill TL. An introduction to statistical thermodynamics. NY: Dover, 1986.
[16] Poland D. Free energy distributions in proteins. Proteins 2001;45:325–36.
[17] He X, Wolkers WF, Crowe JH, Swanlund DJ, Bischof JC. In situ thermal denaturation of proteins in Dunning AT-1 prostate cancer cells and its correlation with hyperthermic cell injury, to be published.
[18] Despa F, Orgill DP, Lee RC. Effects on crowding on the thermal stability of heterogeneous protein solutions. Ann Biomed Eng; submitted.
[19] Makhatadze GI, Privalov PL. Energetics of protein structure. Adv Protein Chem 1995;47:307–425.
[20] Swaminathan R, Hoang CP, Verkman AS. Photobleaching recovery and anisotropy decay of green fluorescent protein GFP-S65T in solution and cells: cytoplasmic viscosity probed by green fluorescent protein translational and rotational diffusion. Biophys J 1997;72:1900–7.
[21] Ellis RJ, Minton AP. Cell biology: join the crowd. Nature 2003;425:27–8.
[22] Minton AP. Effect of a concentrated *inert* macromolecular cosolute on the stability of a globular protein with respect to denaturation by heat and by chaotropes: a statistical–thermodynamic model. Biophys J 2000;78:101–9.
[23] Li J, Zhang S, Wang C. Effects of macromolecular crowding on the refolding of glucose-6phosphate dehydrogenase and protein disulfide isomerase. J Biol Chem 2001;37:34396–401.
[24] Tellam RL, Sculley MJ, Nichol LV, Wills PR. Influence of poly(-ethylene glicol) 6000 on the properties of skeletal-muscle actin. Biochem J 1983;213:651–9.
[25] Eggers DK, Valentine JS. Crowding and hydration effects on protein conformation: a study with sol–gel encapsulated proteins. J Mol Biol 2001;314:911–22.
[26] Miles CA, Burjanadze TV, Bailey AJ. The kinetics of the thermal denaturation of collagen in unrestrained rat tail tendon determined by differential scanning calorimetry. J Mol Biol 1995;245:437–46.
[27] Bischof JC, Padanilam J, Holmes WH, Ezzell RM, Lee RC, Tompkins RG. Dynamics of cell membrane permeability changes at supraphysiological temperatures. Biophys J 1995;68:2608–14.
[28] Borrelli MJ, Wong RS, Dewey WC. A direct correlation between hyperthermia-induced membrane blebbing and survival in synchronous G1 CHO cells. J Cell Physiol 1986;126:181–90.
[29] Filimonov VV, Azuaga AI, Viguera AR, Serrano L, Mateo PL. A thermodynamic analysis of a family of small globular proteins: SH3 domains. Biophys Chem 1999;77:195–208.
[30] Grinberg AV, Gevondyan NM, Grinberg NV, Grinberg VY. The thermal unfolding and domain structure of Na^+/K^+-exchanging ATPase. A scanning calorimetry study. Eur J Biochem 2001;268:5027–36.
[31] Levi V, Rossi JPFC, Echarte MM, Castelo PR, Gonzalez Flecha FL. Thermal stability of the plasma membrane calcium pump. Quantitative analysis of its dependence on lipid-protein interactions. J Membrane Biol 2000;173:215–25.
[32] Ortega A, Becker VM, Alvarez R, Lepock JR, Gozalez-Serratos H. Interaction of D-600 with the transmembrane domain of the sarcoplasmic reticulum Ca^{2+}-ATPase. Am J Physiol Cell Physiol 2000;279:C166–D172.
[33] Wu P, Nakano S, Sugimoto N. Temperature dependence of thermodynamic properties for DNA/DNA and RNA/DNA duplex formation. Eur J Biochem 2002;269:2821–30.
[34] Xia T, SantaLucia J, Burkard Jr ME, Kierzek R, Schroeder SJ, Jiao X, et al. Biochemistry 1998;37:14719–35.
[35] Karantza V, Baxevanis AD, Freire E, Moudrianakis EN. Thermodynamic studies of the core histones: ionic strength and pH dependence of H2A-H2B dimmer stability. Biochemistry 1995;34:5988–96.
[36] Liggins JR, Lo TP, Brayer GD, Nall BT. Thermal stability of hydrophobic heme pocket variants of oxidized cytochrome *c*. Protein Sci 1999;8:2645–54.
[37] Wang Z-Y, Freire E, McCarty RE. Influence of nucleotide binding site occupancy on the thermal stability of the F1 portion of the chloroplast ATP synthase. J Biol Chem 1993;268:20785–90.

[38] Bertazzon A, Tsong TY. Effects of ions and pH on the thermal stability of thin and thick filaments of skeletal muscle: high-sensitivity differential scanning calorimetric study. Biochemistry 1990;29: 6447–52.
[39] Bertazzon A, Tsong TY. High-resolution differential scanning calorimetric study of myosin, functional domains, and supramolecular structures. Biochemistry 1989;28:9784–90.
[40] Menendez M, Rivas G, Fernando Diaz J, Andreu JM. Control of the structural stability of the tubulin dimer by one high affinity bound magnesium ion at nucleotide N-site. J Biol Chem 1998;273: 167–76.
[41] Hill TJ, Lafitte D, Wallace JI, Cooper HJ, Tsvetkov PO, Derrick PJ. Biochemistry 2000;39:7284–90.
[42] Leikina E, Mertts MV, Kuznetsova N, Leikin S. Type I collagen is thermally unstable at body temperature. Proc Natl Acad Sci USA 2002;99:1314–8.
[43] Venugopal MG, Ramshaw JA, Braswell E, Zhu D, Brodsky B. Electrostatic interactions in collagen-like triple-helical peptides. Biochemistry 1994;33:7948–56.
[44] Bhowmick S, Swanlund DJ, Bischof JC. Supraphysiological thermal injury in dunning AT-1 prostate tumor cells. ASME J Biomech Eng 2000;122:51–9.
[45] Dudich IV, Zav'yalov VP, Pfeil W, Gaestel M, Zav'yalova GA, Denesyuk AI, et al. Dimer structure as a minimum cooperative subunit of small heat-shock proteins. Biochim Biophys Acta 1995;11253: 163–8.